

# Electron correlation and Fermi surface topology of $\text{Na}_x\text{CoO}_2$

Sen Zhou<sup>1</sup>, Meng Gao<sup>1</sup>, Hong Ding<sup>1</sup>, Patrick A. Lee<sup>2</sup>, and Ziqiang Wang<sup>1</sup>

<sup>1</sup> *Department of Physics, Boston College, Chestnut Hill, MA 02467 and*

<sup>2</sup> *Department of Physics, Massachusetts Institute of Technology, Cambridge, MA 02139*

(Dated: November 8, 2018)

The electronic structure of  $\text{Na}_x\text{CoO}_2$  revealed by recent photoemission experiments shows important deviations from band theory predictions. The six small Fermi surface pockets predicted by LDA calculations have not been observed as the associated  $e'_g$  band fails to cross the Fermi level for a wide range of sodium doping concentration  $x$ . In addition, significant bandwidth renormalizations of the  $t_{2g}$  complex have been observed. We show that these discrepancies are due to strong electronic correlations by studying the multi-orbital Hubbard model in the Hartree-Fock and strong-coupling Gutzwiller approximation. The quasiparticle dispersion and the Fermi surface topology obtained in the presence of strong local Coulomb repulsion are in good agreement with experiments.

PACS numbers: 71.27.+a, 71.18.+y, 74.25.Jb, 74.70.-b

The cobaltates ( $\text{Na}_x\text{CoO}_2$ ) are doped 3d transition metal oxides in which the Co atoms form a layered hexagonal lattice structure. In contrast to the high- $T_c$  cuprates, where the  $\text{Cu}^{2+}$  has a  $3d^9$  configuration and occupies the highest *single*  $e_g$  ( $d_{x^2-y^2}$ ) orbital near the Fermi level, the cobaltates are *multi-orbital* systems where the  $\text{Co}^{4+}$  is in the  $3d^5$  configuration, occupying the three lower  $t_{2g}$  orbitals, similar to the ruthenates ( $\text{Sr}_2\text{RuO}_4$ ). The unexpected discovery [1] of a superconducting phase of yet unknown origin in hydrated  $\text{Na}_x\text{CoO}_2$  around  $x \sim 0.3$  has generated renewed interests in this material. However, such basic issues as the low energy electronic structure and Fermi surface topology in the cobaltates have not been well understood. Band structure (LDA) calculations [2] find that the trigonal symmetry of the Co site in the triangular lattice splits the three  $t_{2g}$  complex into an  $a_{1g}$  and two degenerate  $e'_g$  states at the zone center ( $\Gamma$  point). The LDA predicts a large Fermi surface (FS) associated with the  $a_{1g}$  band enclosing the  $\Gamma$  point and six small FS pockets of mostly  $e'_g$  character near the K points [2, 3].

However, recent angle-resolved photoelectron spectroscopy (ARPES) measurements on the cobaltates revealed only a *single* hole-like FS centered around the  $\Gamma$  point for a wide range of Na concentration  $x$  [4, 5, 6, 7]. The area enclosed by the FS exhausts the Luttinger volume, which is consistent with the observation that the dispersion of the  $e'_g$  band associated with the LDA FS pockets lies below and never crosses the Fermi level [4]. The absence of the FS pockets is unexpected and puts serious constraints on several proposed theories of non-phonon mediated superconductivity as well as magnetic properties based on the nesting conditions of the FS pockets [8, 9, 10]. Furthermore, the measured quasiparticle bandwidths are significantly narrower than the LDA predictions [4, 5]. These fundamental discrepancies between ARPES and LDA suggest that the effects of strong electronic correlations are important in the cobaltates. The effects of local Coulomb repulsion  $U$  has been con-

sidered in the LSDA+U approach, which indeed finds the absence of the small FS pockets [11]. However, the latter is tied to the fully polarized ferromagnetic state in the LSDA+U theory which gives spin-split bands and a spin polarized FS with an area twice as large. This is inconsistent with ARPES and likely an artifact of the LSDA+U approximation. A recent calculation based on the multi-orbital Hubbard model and the dynamical mean-field theory finds that the FS pockets become even larger in size than the LDA predictions [12].

The focus of the present work is to explain how strong correlations drive orbital polarization and the band narrowing observed in ARPES. We adopt a multi-orbital Hubbard model description where the noninteracting part is determined by fitting the LDA band structure. The interacting part contains both the intra ( $U$ ) and the inter-orbital ( $U'$ ) local Coulomb repulsion as well as the Hund's rule coupling  $J_H$ . First, a basis independent Hartree-Fock (HF) calculation is performed which is in essence a LDA+U calculation in the paramagnetic phase. We find that for  $U'$  much less than  $U$ , multi-orbital occupation is favored in order to reduce the cost of double occupation. As a result, the HF self-energy renormalizes the atomic level spacing in such a way that the size of the FS pockets associated with the  $e'_g$  band grows. This trend is however reversed when  $U'$  grows and becomes comparable to  $U$ . In the HF theory, the size of the  $e'_g$  FS pockets begins to shrink for  $U'/U > 3/5$ . To correctly capture the physics of strong correlation for large  $U$  and  $U'$ , we generalize the Gutzwiller approximation to the case of multi-orbitals. We find that in the strong-coupling regime, orbital polarization is tied to Pauli-blocking, i.e. the orbital occupation dependence of the Gutzwiller band renormalization factors. We obtain both band narrowing and the disappearance of the FS pockets in good agreement with the ARPES experiments.

We start with the multi-orbital tight-binding model on

a two-dimensional triangular lattice,

$$H_0 = - \sum_{ij,\sigma} \sum_{\alpha\beta} t_{ij,\alpha\beta} d_{i\alpha\sigma}^\dagger d_{j\beta\sigma} - \frac{\Delta}{3} \sum_{i,\sigma} \sum_{\alpha\neq\beta} d_{i\alpha\sigma}^\dagger d_{i\beta\sigma}, \quad (1)$$

where the operator  $d_{i\alpha\sigma}^\dagger$  creates an electron in the  $\alpha$  orbital with spin  $\sigma$  on the Co site and  $t_{ij,\alpha\beta}$  is the hopping integral between the  $\alpha$  orbital on site  $i$  and the  $\beta$  orbital on site  $j$ . The relevant valence bands near the FS consist of the Co  $t_{2g} = \{d_{xy}, d_{yz}, d_{zx}\}$  orbitals and have an electron occupancy of  $5 + x$ . The  $\Delta$  in Eq. (1) describes the crystal field due to trigonal distortion that splits the  $t_{2g}$  complex into a lower  $a_{1g}$  singlet and a higher  $e'_g$  doublet, where  $a_{1g} = (d_{xy} + d_{yz} + d_{zx})/\sqrt{3}$ , and  $e'_g = \{(d_{zx} - d_{yz})/\sqrt{2}, (2d_{xy} - d_{yz} - d_{zx})/\sqrt{6}\}$ . For convenience, we will work in the hole-picture via a particle-hole transformation  $d \rightarrow \tilde{d}^\dagger$ , in which the band filling of holes is  $1 - x$ . The structure of the tight-binding Hamiltonian in k-space on the triangular lattice is

$$H_0 = \sum_{k,\sigma,\alpha\beta} \mathbf{K}_{\alpha\beta}^d(k) \tilde{d}_{k\alpha\sigma}^\dagger \tilde{d}_{k\beta\sigma} + \frac{\Delta}{3} \sum_{k,\sigma,\alpha\neq\beta} \tilde{d}_{k\alpha\sigma}^\dagger \tilde{d}_{k\beta\sigma}. \quad (2)$$

The hopping matrix  $\mathbf{K}$  in the  $t_{2g}$  basis is given by

$$\mathbf{K}^d(k) = \begin{pmatrix} \varepsilon(t, 1, 2, 3) & \varepsilon(t', 3, 1, 2) & \varepsilon(t', 2, 3, 1) \\ \varepsilon(t', 3, 1, 2) & \varepsilon(t, 2, 3, 1) & \varepsilon(t', 1, 2, 3) \\ \varepsilon(t', 2, 3, 1) & \varepsilon(t', 1, 2, 3) & \varepsilon(t, 3, 1, 2) \end{pmatrix}, \quad (3)$$

with  $(1, 2, 3) = (k_1, k_2, k_3)$ ,  $k_1 = \sqrt{3}k_x/2 - k_y/2$ ,  $k_2 = k_y$ ,  $k_3 = -k_1 - k_2$ , and  $\varepsilon(t, 1, 2, 3) = 2t_1 \cos k_1 + 2t_2 (\cos k_2 + \cos k_3) + 2t_3 \cos(k_2 - k_3) + 2t_4 [\cos(k_3 - k_1) + \cos(k_1 - k_2)] + 2t_5 \cos(2k_1) + 2t_6 [\cos(2k_2) + \cos(2k_3)] + \dots$ . The  $(t, t')$  denote the (intra,inter)-orbital hopping.

Fig.1 shows the fitting of the tight-binding dispersions obtained by diagonalizing Eq. (2) to the LDA band structure at  $x=1/3$  [3]. We note that the fit with up to third-nearest-neighbor (NN) hopping or more describes the LDA bands quite well. On the other hand, the tight-binding model cannot reproduce completely the LDA dispersions even with up to eighth-NN hopping. The discrepancy is most pronounced along the M-K direction where the two  $e'_g$  bands cross in the tight-binding fit (Fig. 1a). Similar disagreement can be traced back to the previous tight-binding fits [10, 12, 13]. We believe the difficulty arises from the hopping path via the O  $2s$  and  $2p$  orbitals. Nevertheless, the tight-binding model works very well at low energies near the Fermi level. The FS consists of a cylindrical sheet around the  $\Gamma$ -point and six hole pockets near the K-points as shown in Fig. 1b-d. The central FS has a dominant  $a_{1g}$  character while the six FS pockets are mainly of the  $e'_g$  character. The hopping integrals obtained from the fit with up to third-NN are  $t=(-44.6, -9.0, 36.2, 5.9, 57.9, 36.7)$ meV and  $t'=(-157.8, -30.2, 37.1, 9.2, -11.9, -21.0)$ meV. The crystal-field splitting  $\Delta$  is chosen to be 0.01eV. In the rest of the paper,

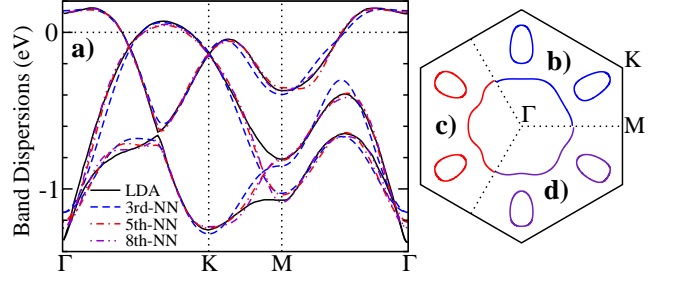


FIG. 1: Tight-binding fits to the LDA band structure at  $x = 1/3$ . (a) The fitted band dispersions with up to 3rd, 5th and 8th NN hopping. The corresponding Fermi surfaces are plotted in (b), (c), and (d) respectively.

we use these parameters for  $H_0$ . Our results are insensitive to these values provided that they provide a good fit of the LDA band structure near the FS. Note that although holes are evenly distributed among the three  $t_{2g}$  orbitals, in the  $a_{1g}$  and  $e'_g$  basis (hereafter referred to as the  $\{a\}$  basis), the hole occupations are 0.123 ( $e'_g$ ) and 0.421 ( $a_{1g}$ ) respectively. Despite its higher orbital energy, the  $a_{1g}$  hole orbital has a higher occupation due to its larger bandwidth.

The correlation effects are described by the multi-orbital Hubbard model  $H = H_0 + H_I$ , where  $H_0$  is the tight-binding Hamiltonian in Eq.(2),  $H_I$  represents the local Coulomb repulsion  $U$  (intra-orbital) and  $U'$  (inter-orbital) and Hund's rule coupling  $J_H$ . For  $t_{2g}$  orbitals,  $H_I$  has been shown to take the form [14]

$$H_I = U \sum_{i,\alpha} \hat{n}_{i\alpha\uparrow} \hat{n}_{i\alpha\downarrow} + (U' - \frac{1}{2}J_H) \sum_{i,\alpha>\beta} \hat{n}_{i\alpha} \hat{n}_{i\beta} \quad (4)$$

$$- J_H \sum_{i,\alpha\neq\beta} \mathbf{S}_{i\alpha} \cdot \mathbf{S}_{i\beta} + J_H \sum_{i,\alpha\neq\beta} a_{i\alpha\uparrow}^\dagger a_{i\alpha\downarrow}^\dagger a_{i\beta\downarrow} a_{i\beta\uparrow}.$$

with  $U' = U - 2J_H$ . Here  $\hat{n}_{i\alpha}$  and  $\mathbf{S}_{i\alpha}$  are the density and the spin operators in the  $\{a\}$  basis where the tight-binding part  $H_0$  is

$$H_0 = \sum_{k,\sigma} \sum_{\alpha\beta} \mathbf{K}_{\alpha\beta}^a(k) a_{k\alpha\sigma}^\dagger a_{k\beta\sigma} + \sum_{k,\alpha,\sigma} \Delta_\alpha a_{k\alpha\sigma}^\dagger a_{k\alpha\sigma}. \quad (5)$$

Here  $\Delta_\alpha = -\Delta/3, 2\Delta/3$  for the  $e'_g$  and  $a_{1g}$  orbitals respectively. The hopping matrix  $\mathbf{K}^a(k) = \mathbf{O}^T \mathbf{K}^d(k) \mathbf{O}$ , with  $\mathbf{O}$  the orthogonal rotation from the  $t_{2g}$  to the  $\{a\}$  basis.  $H_I$  is identical in these two bases. The hierarchy of the interaction strength is  $U > U' > J_H \geq 0$ .

We first study the effects of interactions in the HF theory in the orbital sector. In the paramagnetic phase, the interacting Hamiltonian is given by,

$$H_I^{HF} = \sum_{k,\sigma,\alpha} (\frac{1}{2}U n_\alpha + U'_{\text{eff}} \sum_{\beta\neq\alpha} n_\beta) a_{k\alpha\sigma}^\dagger a_{k\alpha\sigma}$$

$$- \frac{U}{4} \sum_{k,\alpha} n_\alpha^2 - \frac{U'_{\text{eff}}}{2} \sum_{k,\alpha\neq\beta} n_\alpha n_\beta \quad (6)$$

$$+ (U - 2U'_{\text{eff}}) \sum_{k,\alpha\neq\beta} [n_{\alpha\beta} a_{k\alpha\sigma}^\dagger a_{k\beta\sigma} - \frac{n_{\alpha\beta}^2}{2}],$$

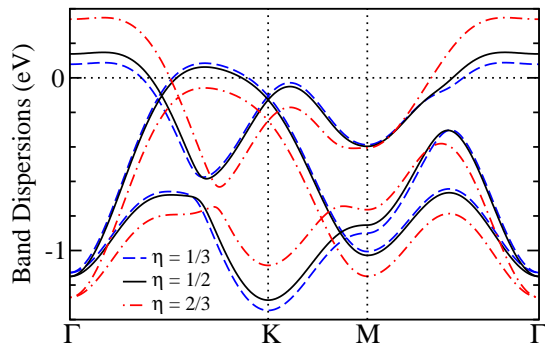


FIG. 2: HF results for  $U = 3.0\text{eV}$  at  $x = 1/3$ . The band dispersions are shown for  $\eta = 1/3, 1/2, 2/3$ .

where  $n_{\alpha\beta} = (1/N_s) \sum_{k,\sigma} n_{\alpha\beta}^{\sigma}(k)$ ,  $n_{\alpha\beta}^{\sigma}(k) = \langle a_{k\alpha\sigma}^{\dagger} a_{k\beta\sigma} \rangle$ ,  $n_{\alpha} = n_{\alpha\alpha}$ , and  $U'_{\text{eff}} = U' - J_H/2$ . In essence, this HF analysis, also discussed in Ref. [12], is equivalent to the LDA+U theory [15]. Since we are interested in the orbital dependent corrections, we have not displayed in Eq. (6) the double-counting term which corrects for the energy already included in the LDA, because it depends only on the total density.

Note that the HF theory is basis independent. It is thus convenient to stay in the  $\{a\}$  basis where the local density matrix, and thus the HF self-energies are diagonal in orbital space, i.e.  $n_{\alpha\neq\beta} = 0$ . Then the average energy has contributions only from the first two terms in Eq. (6). Recall that most of the holes reside in the  $a_{1g}$  orbitals. If  $U'_{\text{eff}} < U/2$ , it is favorable to increase the population of the  $e'_g$  orbitals to take advantage of the smaller inter-orbital repulsion  $U'_{\text{eff}}$ . On the other hand for  $U'_{\text{eff}} > U/2$ , the tendency is to empty the  $e'_g$  orbitals in favor of  $a_{1g}$  occupation. The crucial factor of 1/2 in front of  $U$  comes from the fact that due to exchange, intra-orbital repulsion operates only between holes with opposite spin, whereas both spins contribute to  $U'_{\text{eff}}$ .

We proceed to calculate the HF self-energy in terms of the average  $\bar{n} = (n_{a_{1g}} + 2n_{e'_g})/3 = (1-x)/3$  and the difference  $\delta = (n_{a_{1g}} - n_{e'_g})/3$  between the hole occupation of the  $a_{1g}$  and  $e'_g$  orbitals,

$$\Sigma_{e'_g}^{\text{HF}} = \frac{1}{2}\bar{n}U(1+4\eta) + \delta U(\eta - 1/2) \quad (7)$$

$$\Sigma_{a_{1g}}^{\text{HF}} = \frac{1}{2}\bar{n}U(1+4\eta) - 2\delta U(\eta - 1/2) \quad (8)$$

where  $\eta = U'_{\text{eff}}/U$  is the relative strength of the inter-orbital interaction. The interaction effect in the paramagnetic HF theory is to simply shift the atomic levels by  $\Sigma_{e'_g}^{\text{HF}}$  and  $\Sigma_{a_{1g}}^{\text{HF}}$  respectively, resulting in a renormalization of the atomic level spacing  $\Delta' = -3\delta U(\eta - 1/2)$ . As expected, the direction of the charge transfer depends on the ratio  $\eta$ . Since the majority of the holes resides in the  $a_{1g}$  orbital in the noninteracting limit,  $\delta > 0$ . Thus, for  $\eta < 1/2$ , the level splitting renormalizes upward,  $\Delta' > 0$ , and interactions induce a transfer of carriers from the  $a_{1g}$  to the  $e'_g$  orbital. The self-consistent HF results are

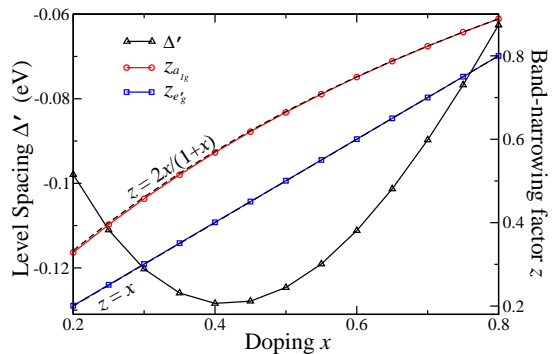


FIG. 3: The doping  $x$  dependence of the level spacing and bandwidth renormalization for the  $a_{1g}$  and  $e'_g$  orbitals.

shown in Fig. 2 at  $x = 1/3$  for  $U = 3\text{eV}$  which is close to the value (3.7 eV) estimated from the LDA [13]. For  $\eta = 1/3$ , the size of the hole pockets indeed becomes larger than that of the noninteracting/LDA ones. At  $\eta = 1/2$ , the self-energy corrections are equal among the orbitals and the noninteracting (LDA) band dispersions are unchanged as shown in Fig. 2. When  $\eta > 1/2$ , i.e. for  $U'/U > 3/5$  or  $J_H/U < 1/5$  which is reasonable for the cobaltates [11], the level splitting renormalizes downward,  $\Delta' < 0$ , triggering a transfer of holes from the  $e'_g$  to the  $a_{1g}$  orbital. The six FS pockets continues to shrink as the  $e'_g$  band sinks with increasing  $\eta$  and disappears beyond a critical ratio  $\eta_c$ , as shown in Fig. 2 for  $\eta = 2/3$ . We find that  $\eta_c(U = 3.0\text{eV}) \simeq 5/8$ .

The HF analysis shows that the disappearance of the six FS pockets near the K-points is the physics of large  $U$  and  $U'$  compared with  $J_H$ . In this case, the HF theory itself becomes unreliable. Moreover, the localization tendency leading to the bandwidth reduction cannot be captured by the HF theory. It is therefore instructive to study the problem in the strong-coupling limit by projecting out the states of double-occupation prohibited by the large on-site Coulomb repulsions. This can be achieved by the Gutzwiller projection  $|\Psi(\{n_{\alpha}\})\rangle = P_G|\Psi_0(\{n_{\alpha}\})\rangle$ , where  $P_G$  is the projection operator that operates on the noninteracting state  $|\Psi_0(\{n_{\alpha}\})\rangle$  in a given orbital occupation scheme  $\{n_{\alpha}\}$ . It removes the double-occupancy by electrons from both the same and different orbitals. This variational procedure is most conveniently implemented in the Gutzwiller approximation where the effect of projection is taken into account by the statistical weighting factor multiplying the quantum coherent state [16]. Specifically, we approximate the hopping term by

$$\langle \Psi | a_{i\alpha\sigma}^{\dagger} a_{j\beta\sigma} | \Psi \rangle = g_t^{\alpha\beta} \langle \Psi_0 | a_{i\alpha\sigma}^{\dagger} a_{j\beta\sigma} | \Psi_0 \rangle, \quad (9)$$

where the Gutzwiller renormalization factor  $g_t$  is given by the ratio of the probabilities in the hopping process in the projected  $|\Psi\rangle$  and the unprojected  $|\Psi_0\rangle$ . We find,

$$g_t^{\alpha\beta} = \frac{x}{\sqrt{(1-n_{i\alpha\sigma})(1-n_{j\beta\sigma})}}. \quad (10)$$

It is important to note that in a multi-orbital system  $g_t^{\alpha\beta}$  depends on the occupation of the orbitals connected by the hopping integral as seen in the denominator in Eq. (10). The latter originates from the Pauli principle. It compensates for the effects of “Pauli-blocking” of double-occupation by electrons in the same quantum states which already operate in the free fermion term on the RHS of Eq. (9), while the numerator  $x$  in Eq. (10) describes the “Coulomb-blocking” due to the large on-site  $U$  and  $U'$ . It turns out that the denominator is crucial for carrier transfer and orbital-polarization in the strong-coupling limit. In the uniform paramagnetic phase,  $g_t^{\alpha\beta} = 2x/\sqrt{(2-n_\alpha)(2-n_\beta)}$ . The orbital occupations are variational parameters determined by minimizing the ground state energy of the Hamiltonian,

$$H_{GW} = \sum_{k,\sigma,\alpha\beta} g_t^{\alpha\beta} \mathbf{K}_{\alpha\beta}^a(k) a_{k\alpha\sigma}^\dagger a_{k\beta\sigma} + \sum_{i,\alpha,\sigma} \Delta_\alpha a_{i\alpha\sigma}^\dagger a_{i\alpha\sigma} + \sum_{i,\alpha} \varepsilon_{i\alpha} \left( \sum_\sigma a_{i\alpha\sigma}^\dagger a_{i\alpha\sigma} - n_{i\alpha} \right), \quad (11)$$

where  $\varepsilon_{i\alpha}$  are the Lagrange multipliers enforcing the occupation  $n_{i\alpha} = \sum_\sigma \langle a_{i\alpha\sigma}^\dagger a_{i\alpha\sigma} \rangle$ . They are determined by the self-consistency equation

$$\varepsilon_{i\alpha} = \varepsilon_\alpha = \frac{1}{2-n_\alpha} \frac{1}{N_s} \sum_{k,\beta,\sigma} g_t^{\alpha\beta} \mathbf{K}_{\alpha\beta}^a \langle a_{k\alpha\sigma}^\dagger a_{k\beta\sigma} \rangle. \quad (12)$$

The RHS of this equation is the derivative of the kinetic energy of band  $\alpha$  with respect to  $n_\alpha$ , and can be understood by the following argument. The transfer of a hole from band  $\alpha$  to  $\beta$  causes the respective bandwidths to decrease and increase by  $\mathcal{O}(1/N_s)$ . However, the kinetic energies of the occupied states in each band are changed by order unity, and this energy difference must be reflected in the equilibrium condition by an energy shift  $\varepsilon_\alpha$ . Thus in contrast to HF theory, there is no energy cost proportional to  $U$ . Instead, both the band-narrowing and the renormalization of the level spacing  $\Delta' = \varepsilon_{a_{1g}} - \varepsilon_{e'_g}$  contribute to the redistribution of holes among the orbitals. In Fig. 3, we show the self-consistently determined band-narrowing factor  $z_\alpha = g_t^{\alpha\alpha}$  and the renormalized level spacing. For orbitals with a larger hole occupation, the bandwidth reduction is smaller and the renormalized band energy is lower, resulting in the transfer of more holes into these bands. The combined effects cause the holes to move out of the  $e'_g$  band into the  $a_{1g}$  band. The calculated band dispersions and the FS topology at  $x = 0.3, 0.5, 0.7$  are shown in Fig. 4 in the strong coupling theory. The corresponding non-interacting case is also shown for comparison. The six hole pockets are completely absent at all levels of sodium doping due to strong correlation, leaving a single hexagonal Fermi surface centered around the  $\Gamma$  point satisfying the Luttinger theorem. This, as well as the band-narrowing due to strong Coulomb repulsion, is in very good agreement with the photoemission experiments [4, 5].

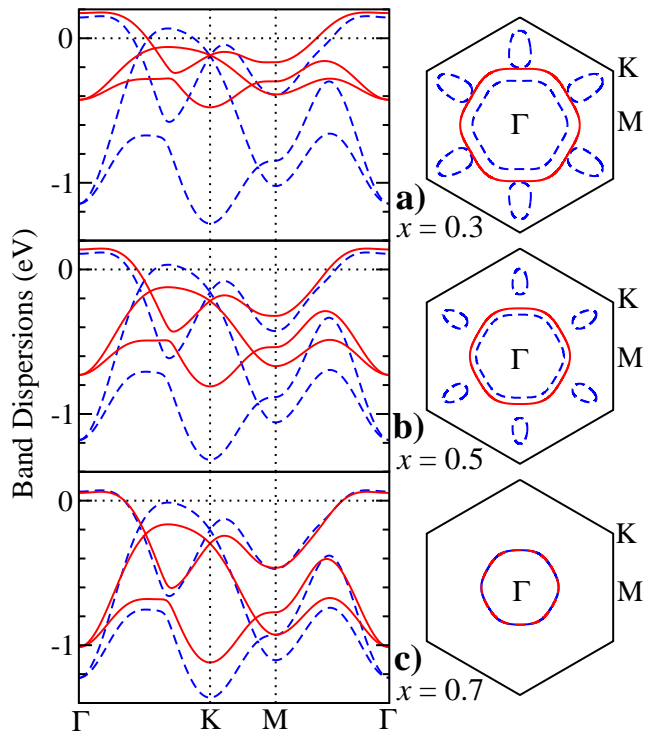


FIG. 4: The band dispersions and the Fermi surfaces in the strong coupling limit (red solid lines) for doping  $x = 0.3, 0.5$  and  $0.7$ . The noninteracting dispersions (blue dashed lines) are also plotted for comparison.

In conclusion, we have shown that strong correlation plays an important role in understanding the electronic structure of  $\text{Na}_x\text{CoO}_2$ . It pushes the  $e'_g$  band below the Fermi level, leading to an orbital polarized state with a single hole-like FS. The absence of the small FS pockets, which would have contributed significantly to the density of states in band structure calculations, further suggests that the large mass enhancement observed in the specific heat measurement [17] is due to strong correlation.

This work is supported by DOE grants DE-FG02-99ER45747 and DE-FG02-03ER46076, ACS grant 39498-AC5M, and NSF grants DMR-0072205 and DMR-0201069.

- 
- [1] K. Takada, et. al., Nature (London) **422**, 53 (2003).
  - [2] D. J. Singh, Phys. Rev. **B61**, 13397 (2000).
  - [3] K.-W. Lee, J. Kuneš, and W. E. Pickett, Phys. Rev. **B70**, 045104 (2004).
  - [4] H. B. Yang, et. al., cond-mat/0501403 (2005).
  - [5] M. Z. Hasan, et. al., cond-mat/0501530 (2005).
  - [6] M. Z. Hasan, et. al., Phys. Rev. Lett. **92**, 246402 (2004).
  - [7] H. B. Yang, et. al., Phys. Rev. Lett. **92**, 246403 (2004).
  - [8] K. Kuroki, Y. Tanaka, and R. Arita, Phys. Rev. Lett. **93**, 077001 (2004).
  - [9] M. D. Johannes, I. I. Mazin, D. J. Singh, and D. A. Papaconstantopoulos, Phys. Rev. Lett. **93**, 097005 (2004).
  - [10] Y. Yanase, M. Mochizuki, and M. Ogata, J. Phys. Soc.

- Jpn. **74**, 430 (2005); M. Mochizuki, Y. Yanase, and M. Ogata, cond-mat/0407094.
- [11] P. Zhang *et al.*, Phys. Rev. Lett. **93**, 236402 (2004); P. Zhang *et al.*, Phys. Rev. **B70**, 085108 (2004).
- [12] H. Ishida, M. D. Johannes, and A. Liebsch, cond-mat/0412654.
- [13] M. D. Johannes, I. I. Mazin, and D. J. Singh, cond-mat/0408696.
- [14] C. Castellani, C. R. Natoli, and J. Ranninger, Phys. Rev. **B18**, 4945 (1978)
- [15] A. I. Liechtenstein, V. I. Anisimov, and J. Zaanen, Phys. Rev. **B52**, R5467 (1995).
- [16] F. C. Zhang, *et al.*, Supercond. Sci. Technol. **1**, 36 (1988).
- [17] F.C. Chou, et. al., Phys. Rev. Lett. **92**, 157004 (2004).